The evaluation of minimum detectable phantom thickness change using a scanning liquid filled ion chamber EPID dose response

M. Mohammadi[1,2,3*] and E. Bezak[1,2]

[1]School of Chemistry and Physics, The University of Adelaide, Adelaide, SA 5000, Australia
[2]Department of Medical Physics, Royal Adelaide Hospital, Adelaide, SA 5000, Australia
[3]Department of Medical Physics, Hamedan University of Medical Sciences, Hamedan, Iran

Background: Although Electronic Portal imaging Devices (EPIDs) have originally developed for positioning verification, they can also be used for dosimetric purposes. In the current work, the dose response of minimum detectable thickness of a Scanning Liquid filled Ion Chamber EPID, SLIC-EPID, and the variation of transmitted dose with the shift of inhomogeneity inside of phantom were investigated. ***Materials and Methods:*** The SLIC-EPID pixel values were converted to the dose values using ionization chamber calibration and KODAK Extended Dose Range films (EDR2 films). The variation of EPID dose values with phantom thickness was investigated. In order to find the rate of dose deposited per centimetre of phantom, several reference points were defined and the variation of dose delivered to the points in the vicinity of reference points was investigated. Two cm thick foam layer, as air gap, was shifted in the beam direction to evaluate the variation of transmitted dose with the shift of inhomogeneity position inside of phantom. ***Results:*** An exponential decrease of the transmitted dose values was observed with the increase of the thickness of attenuators. The maximum and minimum rate of dose deposited per unit of phantom thickness was found to be 5.45% /cm and 3.78% /cm, respectively. Due to the reproducibility and noise level of SLIC-EPID, a 0.5 cm of thickness can be detected with a good reliability. The relative error of EPID dose values increases with an increase of phantom thickness for both data sets. The relative error did not exceed 0.7%. No significant variation in transmitted dose inplane and crossplane profiles were found with the shift of inhomogeneity in the beam direction. ***Conclusion:*** The minimum detectable thickness is an important factor to evaluate an imager for dosimetric purposes. The SLIC-EPID can be used as a reliable two-dimensional dosimeter. **Iran. J. Radiat. Res., 2005; 3 (1): 3-10**

Keywords: *Dose verification, Electronic Portal Imaging Devices, portal dosimetry, transmitted dosimetry.*

INTRODUCTION

Attempts have been made recently to replace traditional methods of portal image acquisition using films with Electronic Portal Imaging Devices (EPIDs). Verification of the geometry of the irradiated fields is faster using EPIDs and the acquired digital images can be analysed on/off line[1, 2]. In addition, EPIDs can be used for dosimetric purposes[3-12]. In order to use Electronic Portal Images (EPIs) for transmitted dosimetry, the relationship between EPID pixel values, dose rate and dose delivered to the EPID sensitive layer was investigated[10, 13-15].

The relationship between EPI pixel values and the attenuator thickness was evaluated and an exponential attenuation of the pixel values with increasing attenuation thickness on the central axis was reported[16]. Converting the EPI pixel values to dose values, the relationship between transmitted dose values, measured using EPID, and phantom thickness was investigated on the central axis[8, 14]. The relationship between ionization current, obtained from ion chamber measurements, and EPID pixel values was investigated and the relationship between transmitted dose values and a range of phantoms with different thicknesses and materials was reported[10]. The maximum deviation of SLIC-EPID pixel values for two photon energies (6 and 10 MV) for perspex, aluminium and lead were found to be 2%, 3% and 2.1% respectively. Defining the observed deviation factor as $(G/D)/(G/D_{average})$, where G is the measured pixel grey value and D is the dose, the dependence of EPID detector response as a function of patient thickness was investigated and a linear decrease in the corrected EPID response with the increase of absorber thickness was observed[11]. The variation of EPID pixel values with the increase of the thickness of the lead attenuator on the central axis of radiation

Corresponding author:
Mohammad Mohammadi, Department of Medical Physics, Royal Adelaide Hospital, Adelaide, SA 5000, Australia
Fax: *+61 8 82225937*
E-mail: *MMohamma@mail.rah.sa.gov.au*

field was reported[8]. Menon *et al*, in a study of compensator quality control procedures with an amorphous silicon EPID showed that variation of the EPID response in the presence of attenuators in the beam path for a field size 20 × 20 cm² at SSDs of 105 cm and 140 cm, could be fitted with exponential curves[17].

Although the correlation between transmitted dose, measured with different types of commercial EPIDs, and patient/phantoms thickness has been reported, it is not clear that what range of patient/phantom thickness can be detected with an acceptable reliability. Moreover, the minimum detectable change of patient/phantom thickness, occurring as a result of organ motion or due to spatial shifts, has not been investigated.

In this work, experimental data was collected to investigate the dosimetric properties of EPIDs in the presence of homogeneous and inhomogeneous phantoms. Firstly, the variation of measured transmitted dose in the EPID with the increase of a homogeneous phantom thickness on the central axis was investigated. The relationship between transmitted dose and SLIC-EPID pixel values was investigated and the rate of transmitted dose variation with the change of phantom thickness was investigated for a range of phantom thicknesses. Several phantom thicknesses were selected as reference and the rate of dose variation per 1 centimetre of phantom thickness was investigated. Secondly, the effect of inhomogeneity position in the direction of radiation beam was also investigated.

MATERIALS AND METHODS

SLIC-EPID and linac

The digital portal imager used in this study is a SLIC-EPID (LC250, Varian Oncology Systems, Palo Alto, CA), incorporated in Varian 600CD linac. It consists of 256×256 detectors. The size of each chamber and the whole sensitive area are 1.27×1.27×1 mm³ and 32.5×32.5 cm², respectively. The polarizing voltage (400 V) is applied to each row. The ionization chamber currents in all columns are measured and recorded as pixel values. EPID images were acquired in fast read-out and full resolution mode. In this work, each EPID pixel value matrix is the average of two consecutively acquired images with pixel values standard deviation of less than 1%[18].

All EPID measurements were performed using the Varian 600CD linear accelerator (linac) equipped with 80-leaf MLC, Enhanced Dynamic Wedges (EDW), and SLIC-EPID. The linac produces 6 MV photon beam with dose rates from 100 to 600 MU/min. Image acquisition was performed using available repetition modes, with one monitor unit corresponding to a calibrated dose delivery of 1 cGy (1 rad) in the reference conditions.

Several experiments were designed to evaluate the EPID response in the presence of various phantom thicknesses. In the first stage, as figure 1-a illustrates, the thickness of phantom was varied from 0 cm to 28 cm. Two consecutive images were acquired and averaged for each measurement set up at a Source to EPID Distance (SED) = 140 cm for a 10× 10 cm² field size, with repetition rate of 300 MU/min. To increase the accuracy of transmitted dose, extra build up layer on the surface of EPID cover is required[4, 13, 14]. The thickness of extra build-up layer to reach the electronic equilibrium was determined 5 mm of white water, RW3,(ρ = 1045 g/cm³, PTW Freiburg) material[19]. The experiment was performed with and without 5 mm of RW3 material on the top of EPID cover. The SLIC-EPID pixel values on the central axis were calibrated using the dose values measured by an ion chamber under the same conditions. The EPID pixel values were converted to the dose values using the equation:

$$D = a(PV)^b \qquad (1)$$

Where D is the transmitted dose delivered to the central axis on the EPID sensitive layer, and PV is EPID pixel value. a and b are two constants dependant on the setting of the EPID, the linac repetition mode, and EPID calibration procedure. A 10×10 pixel matrix was selected as the POI on the central axis. The area represented by this pixel array is 0.90 ×0.90 cm² at the isocentre and 1.27×1.27 cm² at the EPID sensitive layer. This array size was chosen to minimize statistical fluctuation in pixel response with enough spatial resolution[16]. The experiment was also performed without extra build-up layer under the same conditions. The variation of transmitted dose values obtained from EPID

pixel values were then investigated versus the position of calibration point in the phantom.

The standard manufacturer of SLIC-EPID produces uniform response images for patient position verification. As a result, Correction Factor Matrix (CFM) was defined in order to relate two-dimensional EPID relative dose values to corresponding EDR2 film relative dose values:

$$CFM_{i,j} = \frac{D_{i,j}(EDR2\ film)}{D_{i,j}(EPID)} \qquad (2)$$

Where $CFM_{i,j}$ is the spatial CFM values, $D_{i,j}$ (EDR2 film) and $D_{i,j}$ (EPID) are spatial EDR2 film and EPID dose values, respectively. The relative absorbed dose to water at all points of acquired EPID images was calculated as follows:

$$D_{i,j}\ (EPID\ \ Corrected\ ) = D_{i,j}\ (EPID\ \ Measured\ ) \times CFM_{i,j} \qquad (3)$$

Next, the variation of EPID pixel value with the shift of inhomogeneity position in the direction of radiation beam was investigated. Two cm thick foam layer was used to simulate an air gap. It was initially located on the top of 18 cm thick solid water phantom. The position of the air gap was then shifted through the phantom in 2 cm steps, moving the air gap inhomogeneity from the top to the bottom of 18-cm solid water phantom (see figure 1-b). The EPID pixel values were converted to the dose values using equation 1. The radiation profiles were normalized to the value on the central axis for a 10×10 pixel matrix. The Region Of Interest (ROI) was selected in measured dose maps surrounded by the 50% isodose line image boundary using a MATLAB in-house code (MATLAB 6.5.1 Mathworks Inc.).

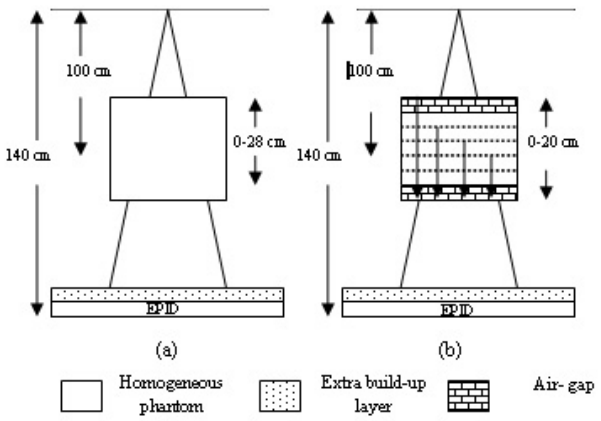

Figure 1. Schematic view of the measurement set-up to evaluate the EPID response versus the phantom thickness. (a) Experimental set-up for EPID response for various thicknesses of homogeneous phantom. (b) Experimental set-up for EPID response for various positions of 2 cm air gap inhomogeneity.

RESULTS

Prior the conversion of EPI pixel values to the dose values, the EPI pixel values acquired with and without build-up layer was compared. A near constant difference in EPID pixel values was observed (approximately 21.85 ± 2.15). Similar results were observed in the absence of phantom (approximately 23.5 ± 2.75).

The relationship between transmitted dose values, measured using a SLIC-EPID, and phantom thickness is shown in figure 2. The x and y axes represent dose values (cGy) and phantom thickness (cm), respectively. As expected[8, 14], an exponential decrease in the EPID dose values with the increase of phantom thickness was observed for both with and without extra build-up layer ($y = 0.2863e^{-0.0448x}$; R-squared value = 0.9993 and $y = 0.2849e^{-0.0454x}$; R-squared value = 0.9998, respectively).

In order to investigate the variation of relative dose with the change of phantom thickness, the central point of 10 cm thick homogeneous phantom was selected as reference point. The variation of transmitted dose, measured using EPID, with the increase and decrease of phantom thickness was then investigated. This is shown in figure 3 for a range of phantom thicknesses.

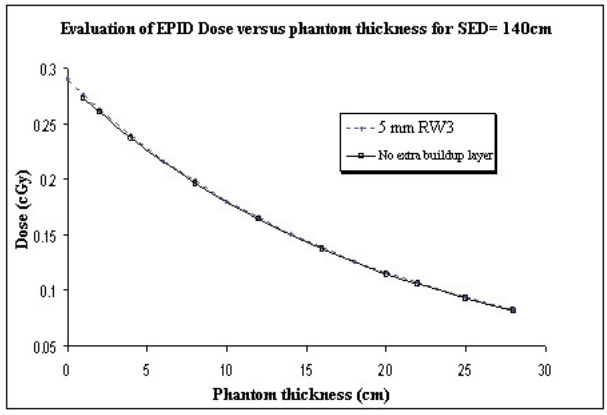

Figure 2. The variation of transmitted dose with the increase of a homogeneous phantom thickness on the central axis using 6 MV photon energy for a 10×10 cm^2 field size, at SED=140 cm and dose rate 300 MU/min. All EPID images were acquired in fast read-out and full resolution mode. Each point is the average of two consecutive measurements.

The x and y axes represent the distance from the reference point and the percentage of the relative dose difference, respectively. It was found that the relative transmitted dose on the central axis decreases 7.01% with the increase of phantom thickness from 1 cm to 2 cm. On the other hand, the relative dose transmitted on the EPID sensitive layer decreases 2.95% with the increase of phantom thickness from 19 cm to 20 cm. On average, the variation of relative dose delivered to the EPID sensitive layer with the increase of phantom thickness by 1 cm was found to be 4.16%.

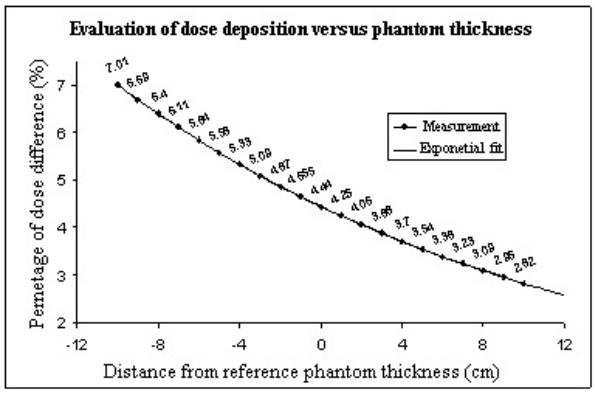

Figure 3. The variation of relative EPID dose with the increase of phantom thickness.

The variation of transmitted dose measured in the EPID sensitive layer with the increase of phantom thickness is not linear. In order to describe this relationship in greater detail, the variation of dose delivered to the various phantom thicknesses was investigated. Several typical thicknesses were selected as reference phantoms (6, 10, 16, 20 and 25 cm thick homogeneous phantom). The variation of relative transmitted dose with the increase/decrease of phantom thickness, (±4 cm), was then investigated. The results are shown in figure 4 for a range

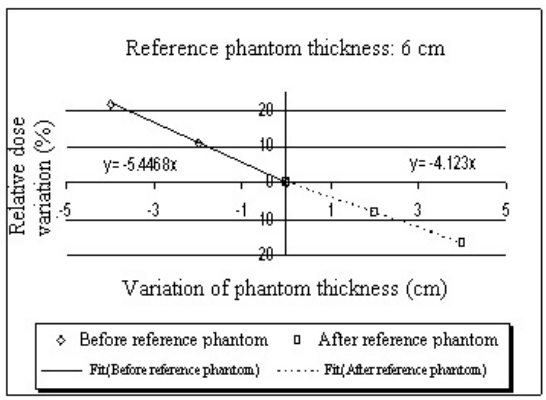

(a)

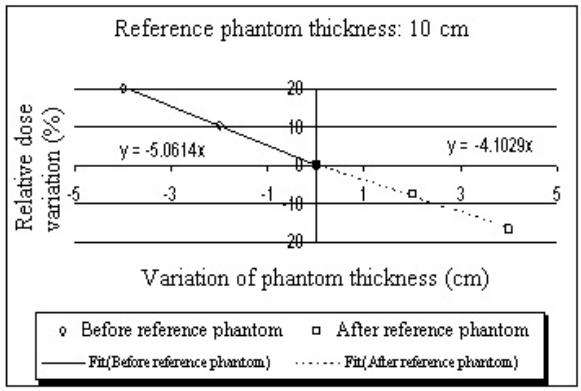

(b)

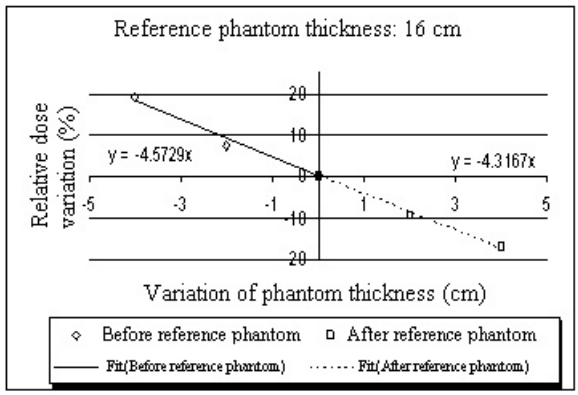

(c)

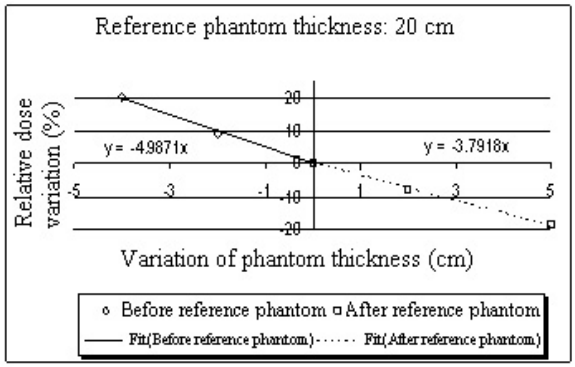

(d)

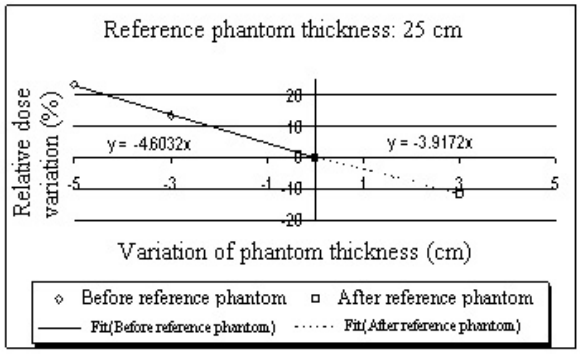

(e)

Figure 4. The variation of relative transmitted dose versus the change of phantom thickness for several defined reference phantom thicknesses: (a) 6 cm, (b) 10 cm, (c) 16 cm (d) 20 cm, and (e) 25 cm.

of reference phantoms. The x and y axes represent the variation of phantom thickness and the relative transmitted dose difference, respectively. To estimate the relative transmitted dose variation versus the change of phantom thickness, linear fits and the related equations were added to the graphs. Although the linear function does not represent the most precise fit to the data, it can be used to estimate the relative dose difference for a given change of phantom thickness from the reference phantom.

The relative error, defined as the ratio of the calculated standard deviation and the EPID average dose value for a 10×10 pixel matrix in the centre of radiation field, increases with the increase of phantom thickness with and without the use of extra build-up layer. The variation of relative error of transmitted dose measured using an EPID with the increase of phantom thickness is shown in figure 5. The x and y axes represent the phantom thickness and relative error of transmitted dose values, respectively. The relative error of EPID dose values increases with an increase of phantom thickness for both data sets. The relative error did not exceed 0.7%.

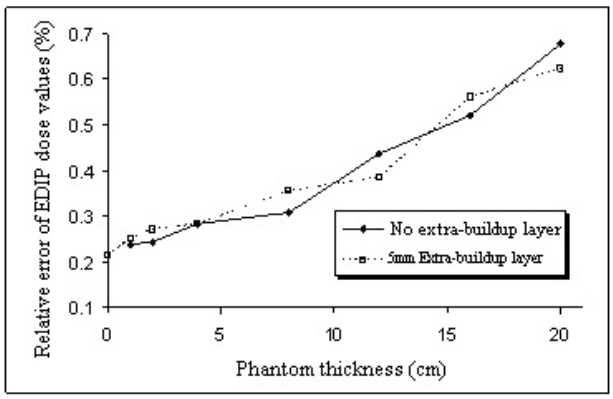

Figure 5. Variation of relative error of EPID dose values on the central axis with the increase of phantom thickness.

To evaluate the impact of air-gap position on the transmitted dose values, measured with EPID, the variation of transmitted dose on the central axis with the change of air-gap position was investigated. The EPID images, acquired for a solid water phantom with incorporated air-gap in the different position along the central axis, were analysed to determine the average pixel value of an array of 8×8 pixels around the beam central axis. The area represented by this pixel array is 0.72 ×0.72 cm² at the isocentre and 1×1 cm² at the EPID sensitive layer. The transmitted dose values measured for 10 various air-gap positions, were normalized relative to the first measurement. The results are shown in figure 6. The x and y axes represent the distance of the centre of the air-gap from an 18 cm thick homogeneous phantom surface and relative dose values, respectively. No significant variation was observed in the transmitted dose values with the change of air-gap geometry inside of phantom.

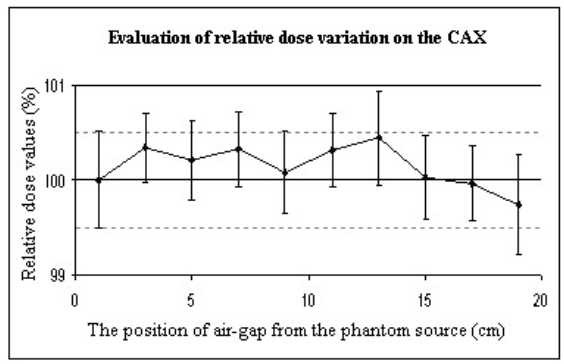

Figure 6. Variation of transmitted dose values with the change of a 2 cm air-gap position inside of an 18 cm homogeneous phantom. Each point is the average of two 8×8 pixel matrices on the central axis, obtained for two EPID images acquired consecutively in fast read-out and full resolution mode for a 6 MV photon beam, a 10×10 cm² field size, 300 MU/min, and SED=140 cm.

Due to the equal total effective path of radiation beam passing through the phantom for all measured geometries, the measured transmitted dose cannot provide information on the position of inhomogeneity in the beam direction. The variation of beam quality for inhomogeneity position leads to the variation of scattered photons. However, due to the large air gap between phantom and portal imager, the difference can be ignored.

The relative transmitted dose inplane and crossplane profiles acquired for a range of air-gap positions are shown in figure 7. The x and y axes represent the distance from the central axis and relative transmitted dose, respectively. Although several fluctuations were observed in the left part of crossplanes, no systematic or significant variations were observed between inplane and crossplane profiles acquired for different positions of 2 cm air gap.

DISCUSSION

The transmitted dose values vary with several factors such as photon intensity, the

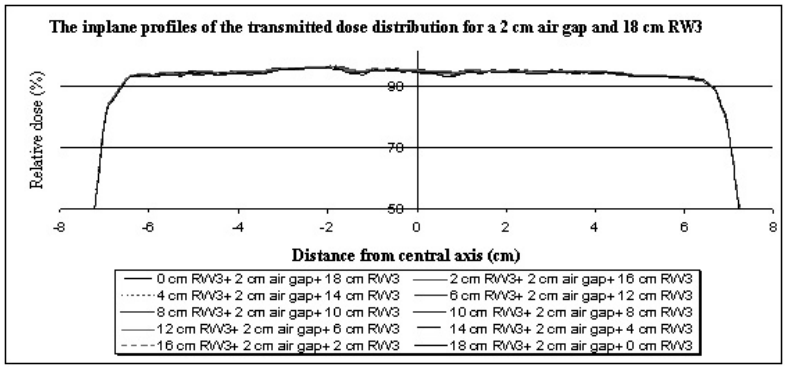

(a)

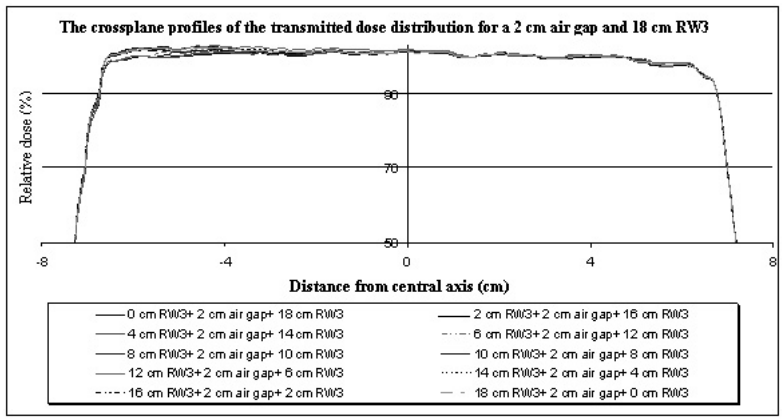

(b)

Figure 7. (a) Inplane profiles of the transmitted dose map using a SLIC-EPID with various position of 2 cm air gap within the 18 cm RW3 phantom. (b) Crossplane profiles of the transmitted dose map using a SLIC-EPID with various position of 2 cm air gap within the 18 cm RW3 phantom. All data are the average of two consecutive EPID images acquired with 6 MV photon energy beam, 300 MU/min, 10×10 cm^2 field size and SED= 140 cm.

distance between source and measurement points, phantom thickness, etc. The relationship between transmitted dose variations with change of phantom thickness is not linear[5, 8, 16, 17]. The minimum detectable phantom thickness using transmitted dose measurements is a factor which depends on the accuracy of device used for transmitted dose measurements. This property will determine the reliability of the system to the change of patient/phantom shifts during the course of treatment.

The EPID dose values in the presence of homogeneous phantoms can be used for dosimetric purposes. The shape of curve and equations obtained in this work, were in agreement with curves and equations reported by Menon *et al.* and Zhu *et al.*, respectively. The differences between coefficients introduced by Menon *et al.* and this work (the a and b constants are 0.4749 and 0.2180 in the $y=a.exp(-bx)$ equation) can be due to different calibration procedures, and different modes of image acquisition. In contrast, the data reported by Zhu *et al.* is based on the decrease of SLIC-EPID raw pixel values with the attenuator thickness and the results can not be compared with those approached in the current work, due to the conversion of SLIC-EPID pixel values conversion to the dose values[8].

As the percentage of dose deposition per centimetre is approximately 4%/cm especially in the thicker phantoms, the EPID calibration should be performed with high precision (less than 1% is recommended)[4, 19]. If uncertainty of physical characteristics, reproducibility and noise level exceeds 1%, the uncertainty of minimum detectable thickness of phantom will increase. In conclusion, EPID can be used as a reliable point-dosimeter if original pixel values are changed to the dose values.

Due to the noise level of SLIC-EPID, approximately 1%[4, 11, 19, 20], and the transmitted dose values measured in this work a 5 mm

change of phantom thickness can be detected using SLIC-EPID. The uncertainty of detection increases with the increase of phantom thickness, because the dose deposition depends exponentially on the phantom thickness. For example, for the thinner phantoms the data variation is smaller than that compared to thicker phantoms.

As figure 4a shows, the variation of relative transmitted dose with the change of reference phantom thickness is not linear. For instance, in a typical reference phantom , 6 cm thick, the rate of relative dose delivered to the phantom per centimetre before and after the reference point are 5.45% /cm and 4.12% /cm, respectively. The increase of beam quality with depth and exponential attenuation are the main reasons for the variation of dose deposited in different thicknesses. In the other words, the low energy photons are absorbed in upper layers of phantom and lower layers interact with harder X-rays.

With the increase of phantom thickness, the probability of Compton effect will increase. As a result, these can increase the probability of scattered photons. With the increase of scattering component, the uncertainty of dose measurement will increase. This is one of the reasons for the increase of relative error of EPID dose values with the increase of phantom thickness. The maximum relative error in this work was found to be 0.7 %. This is an acceptable relative error compared to other published data, e.g. 2% in the work of Parsaei *et al.*[10].

As figures 6 and 7 show, the position and shift along central axis of inhomogeneity inside of phantom cannot be detected using portal images. Although the inhomogeneity in the upper parts of phantom are encountered with soft X-rays comparing with those that are located in the lower parts, the total effective path for the radiation beam is same for all the measurement conditions. For more information about inhomogeneity position in the phantom, other methods and techniques should be used.

CONCLUSION

To evaluate the SLIC-EPID response for dosimetric purposes, the variation of EPI dose values inside of a phantom was investigated. EPI dose values decreases exponentially with the increase of phantom thickness. A good exponential fit was obtained for dose values measured using a SLIC-EPID as function of phantom thickness. The variation of dose deposition in the range of phantom depths was also investigated. The EPID dose values delivered to the phantom in different thicknesses was not linear. Several points in different depths were selected to find the minimum recognisable thickness in the phantom. The results showed that a 5 mm thickness in various thicknesses of phantom, on average, can be detected using EPID dose values deposited to the phantom.

ACKNOWLEDGMENT

One of us (MM) gratefully acknowledges the Iranian Ministry of Health and Medical Education for scholarship of PhD study and financial support.

REFERENCES

1. Antonuk L (2002) Electronic portal imaging devices: a review and historical perspective of contemporary technologies and research. *Phys Med Biol,* ***47****: R31-R56.*
2. Boyer AL, Antonuk L, Fenster A, van Herk M, Meertens H, Munro P, *et al*. (1992) A review of electronic portal imaging devices (EPIDs). *Med Phys,* ***19****: 1-16.*
3. Takai M and Kaneko M (1991) Dosimetric verification using a fluoroscopic portal imaging device. *Med Biol Eng Comput,* ***29 (Suppl)****: 860.*
4. van Herk M (1991) Physical aspects of a liquid filled ionization chamber with pulsed polarizing voltage. *Med Phys,* ***18****: 692-702.*
5. Essers M, Hoogervorst B, van Herk M, Lanson H, Mijnheer B (1995) Dosimetric characteristics of a liquid-filled electronic portal imaging device. *Int J Radiat Oncol Biol Phys,* ***33****: 1265-72.*
6. Heijmen BJ, Pasma KL, Kroonwijk M, Althof VG, de Boer JC, Visser AG, *et al*. (1995) Portal dose measurement in radiotherapy using an electronic portal imaging device (EPID). *Phys Med Biol,* ***40****: 1943-55.*
7. Kirby M and Williams P (1995) The use of an electronic portal imaging device for exit dosimetry and quality control measurements. *Int J Radiat Oncol Biol Phys,* ***31****: 593-603.*
8. Zhu Y, Jiang X, Van Dyk J (1995) Portal dosimetry using a liquid ion chamber matrix: Dose response studies. *Med Phys,* ***22****: 1101-1106.*
9. Symonds-Tayler JRN, Partridge M, Evans PM (1997) An electronic portal imaging device for transit dosimetry. *Phys Med Biol,* ***42****: 2273-2283.*
10. Parsaei H, el-Khatib E, Rajapakshe R (1998) The use of an electronic portal imaging system to measure portal dose and portal dose profiles. *Med Phys,* ***25****: 1903-9.*
11. He X, Van Esch A, Reymen R, Huyskens D (1999) Evaluation of an electronic portal imaging device for transit dosimetry. *Acta Oncol,* ***38****: 591-6.*

12. Grein EE, Lee R, Luchka K (2002) An investigation of a new amorphous silicon electronic portal imaging device for transit dosimetry. *Med Phys,* ***29****: 2262-8.*
13. Boellaard R, van Herk M, Mijnheer BJ (1996) The dose response relationship of a liquid-filled electronic imaging device. *Med Phys,* ***23****: 1601-11.*
14. Essers M, Boellaard R, van Herk M, Lanson H, Mijnheer B (1996) Transmission dosimetry with a liquid- filled electronic portal imaging device. *Int J Radiat Oncol Biol Phys,* ***34****: 931-941.*
15. Greer P and Popescu C (2003) Dosimetric properties of an amorphous silicon electronic portal imaging device for verification of dynamic intensity modulated radiation therapy. *Med Phys,* ***30****: 1618-27.*
16. Roback D and Gerbi B (1995) Evaluation of electronic portal imaging device for missing tissue compensator design and verification. *Med Phys,* ***22****: 2029-34.*
17. Menon GV and Sloboda RS (2003) Compensator quality control with an amorphous silicon EPID. *Med Phys,* ***30****: 1816-24.*
18. Yin F, Schell M, Rubin P (1994) Input/output characteristics of a matrix ion-chamber electronic portal imaging device. *Med Phys,* ***21****: 1447-54.*
19. Mohammadi M, Bezak E (2005) The physical characteristics of a SLIC-EPID for transmitted dosimetry. *Iran J Radiat Res,* ***2****: 175-183.*
20. Louwe R, Tielenburg R, van Ingen K, Mijnheer B, van Herk M (2004) The stability of liquid-filled matrix ionization chamber electronic portal imaging devices for dosimetry purposes. *Med Phys,* ***31****: 819-27.*